

Multiple Parton Scattering in Nuclei: Modified DGLAP Evolution for Fragmentation Functions

Wei-Tian Deng^{1,2} and Xin-Nian Wang²

¹*School of Physics, Shandong University, Jinan, Shandong 250100, China.*

²*Nuclear Science Division, MS 70R0319, Lawrence Berkeley National Laboratory, Berkeley, California 94720*

(Dated: October 22, 2018)

Within the framework of generalized factorization of higher-twist contributions to semi-inclusive cross section of deeply inelastic scattering off a large nucleus, multiple parton scattering leads to an effective medium-modified fragmentation function and the corresponding medium-modified DGLAP evolution equations. We extend the study to include gluon multiple scattering and induced quark-antiquark production via gluon fusion. We numerically solve these medium-modified DGLAP (mDGLAP) evolution equations and study the scale (Q^2), energy (E), length (L) and jet transport parameter (\hat{q}) dependence of the modified fragmentation functions for a jet propagating in a uniform medium with finite length (a “brick” problem). We also discuss the concept of parton energy loss within such mDGLAP evolution equations and its connection to the modified fragmentation functions. With a realistic Wood-Saxon nuclear geometry, we calculate the modified fragmentation functions and compare to experimental data of DIS off large nuclei. The extracted jet transport parameter at the center of a large nucleus is found to be $\hat{q}_0 = 0.024 \pm 0.008 \text{ GeV}^2/\text{fm}$.

PACS numbers: Valid PACS appear here

Keywords:

I. INTRODUCTION

Jet quenching or the suppression of large transverse momentum spectra [1] can be used as an effective probe of the properties of dense medium created in high-energy heavy-ion collisions. Because of multiple scattering and induced gluon bremsstrahlung, an energetic parton propagating in dense medium will lose a significant amount of energy [2–7] and therefore soften its final fragmentation functions. These modified fragmentation functions will lead to the suppression of large transverse momentum single hadron spectra [8, 9], photon-hadron correlations [10–15] both away-side [16, 17] and same-side dihadron correlations [18] in high-energy heavy-ion collisions. Such proposed phenomena have indeed been observed in experiments [19–23] at the Relativistic Heavy-ion Collider (RHIC). Phenomenological studies of the observed jet quenching phenomena at RHIC indicate a scenario of strong interaction between energetic partons and the hot medium with an extremely high initial parton density [16, 24–27]. The same phenomena are also predicted in deeply inelastic scattering (DIS) off large nuclei when the struck quark propagates through the target nuclei [28] though the extracted parton density in cold nuclei is much smaller than that in the hot matter produced in the central $Au + Au$ collisions at RHIC.

Large transverse momentum hadrons in high-energy nucleon-nucleon collisions are produced through hard parton scattering with large transverse momentum transfer and the subsequent fragmentation of energetic partons into final hadrons. Because of the large transverse momentum transfer involved the single inclusive, dihadron and gamma-hadron cross section at large transverse momentum can be calculated within the collinear factorized parton model of perturbative QCD (pQCD) [29–31]. Since the initially produced partons are extremely virtual they will have to go through a cascade of vacuum gluon bremsstrahlung before the final hadronization at a scale $Q_0^2 \sim 1 \text{ GeV}^2$ below which pQCD is no longer valid. In the leading logarithmic approximation, the transverse momenta of the emitted gluons are ordered and therefore each successive gluon emission will contribute to one power of a logarithmic factor $\ln(Q^2/Q_0^2)$ which will counter the small $\alpha_s(Q^2)$ for large momentum scale Q^2 . The resummation of these vacuum gluon bremsstrahlung will lead to a scale dependence of the jet fragmentation functions which can be described by the Dokshitzer-Gribov-Lipatov-Altarelli-Parisi (DGLAP) [32] evolution equations in pQCD.

In the presence of nuclear and hot QCD medium, the initially produced energetic partons will have to go through multiple scattering and induced gluon bremsstrahlung as they propagate through the medium and before hadronization. The induced gluon bremsstrahlung effectively reduces the leading parton’s energy and softens the final hadron spectra or parton fragmentation functions. Within the framework of generalized factorization of higher-twist contribution from multiple parton scattering, one can cast the modification of the semi-inclusive hadron cross section due to multiple parton scattering and induced gluon bremsstrahlung in terms of the effective medium modified parton fragmentation functions [6, 7]. In the same spirit of the vacuum gluon bremsstrahlung, a medium modified DGLAP (mDGLAP) equation was also derived in Refs. [6, 7] which in effect resums successive induced gluon bremsstrahlung due to multiple scattering. The form of the mDGLAP evolution equation is the same as in the vacuum except that the effective splitting functions will contain both vacuum bremsstrahlung and the medium induced parts which should

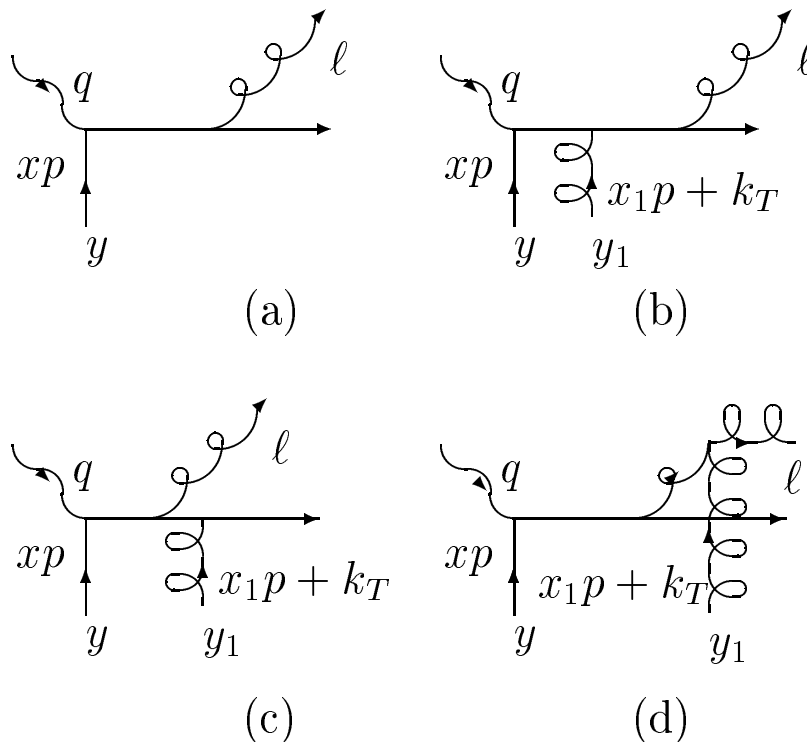


FIG. 1: Gluon radiation from a single scattering (a) and double scattering (b-d) in DIS off a nucleus.

contain information about the properties of the medium as probed by the energetic parton.

Resummation of medium induced gluon bremsstrahlung in terms of a Monte Carlo simulation of parton shower has been carried out [34, 35] within the framework of opacity expansion for induced gluon bremsstrahlung [4], which is equivalent to solving the mDGLAP evolution equations. The mDGLAP evolution equations as derived in the higher-twist approach [6, 7] have also been recently studied numerically [36] for modified fragmentation function in DIS off nuclear targets as this work is being completed.

In this paper, we will extend the mDGLAP evolution equations as derived in Refs. [6, 7] to include both induced gluon bremsstrahlung and induced quark-antiquark pair production from gluon-medium interaction within the same higher-twist expansion approach. We will then solve the coupled mDGLAP evolution equations for gluon and quark fragmentation functions using a numerical method based on Runge-Kutta iteration. We will first consider parton propagation in a uniform medium with finite length and a constant gluon density (so-called "brick" problem). We will study in detail how the modified fragmentation function from mDGLAP evolution equations depend on the initial parton energy, the momentum scale, medium length and the jet transport parameter (or gluon density). Since the concept of parton energy loss becomes ambiguous in the process of successive gluon bremsstrahlung and quark-antiquark pair production, we will consider the singlet quark distribution within a propagating jet with the initial condition of a $\delta(1-z)$ and a given flavor. We will study the momentum fraction carried by the singlet quark distribution function of the fixed flavor and compare to the quark energy loss as calculated in the traditional picture of induced gluon bremsstrahlung. With a realistic Wood-Saxon geometry of cold nuclear matter, we then calculate the nuclear modified quark fragmentation functions from the mDGLAP evolution equations in the DIS off nuclei and compare to experimental data to extract the jet quenching parameter in cold nuclear matter.

II. MODIFIED FRAGMENTATION FUNCTIONS

In DIS off a nucleus target, the struck quark via photon-nucleon interaction is likely to scatter with another nucleon along its propagation path inside the nucleus. Such secondary quark nucleon scattering can also be accompanied by induced gluon bremsstrahlung as illustrated in Figs. 1(b)-(d). The induced gluon bremsstrahlung effectively reduces the energy of the leading quark jet and leads to a medium modified quark fragmentation function. We will work in collision frame where the momentum of virtual photon, the momentum of target nucleus per nucleon and the radiated

gluon are, respectively,

$$\begin{aligned} q &= [-Q^2/2q^-, q^-, \vec{0}_T], \\ p &= [p^+, 0, \vec{0}_T], \\ l &= [l_T^2/2zq^-, zq^-, \vec{l}_T], \end{aligned} \quad (1)$$

and the Bjorken variable is $x_B = Q^2/2q^-p^+$. In this paper, we will use the convention for light-cone momentum (p) and coordinate (y) variables

$$p = [p^+, p^-, \vec{p}_T], \quad p^+ = p_0 + p_z; \quad p^- = (p_0 - p_z)/2, \quad (2)$$

$$y = [y^+, y^-, \vec{y}_T], \quad y^+ = t + z; \quad y^- = (t - z)/2. \quad (3)$$

Within the framework of a generalized factorization of higher-twist contribution to the semi-inclusive cross section from multiple parton scattering, medium modification to the quark fragmentation function was obtained from the double scattering in Figs. 1(b)-(d), the interference between single and triple parton scattering and the corresponding virtual corrections [6, 7, 37],

$$\begin{aligned} \Delta D_q^h(z_h, Q^2) &= \int_0^{Q^2} \frac{dl_T^2}{l_T^2} \frac{\alpha_s}{2\pi} \int_{z_h}^1 \frac{dz}{z} [\Delta\gamma_{q \rightarrow qg}(z, x_B, x_L, l_T^2) D_q^h(z_h/z, Q^2) \\ &\quad + \Delta\gamma_{q \rightarrow gq}(z, x_B, x_L, l_T^2) D_{g \rightarrow h}(z_h/z, Q^2)], \end{aligned} \quad (4)$$

where $D_q^h(z, Q^2)$ and $D_{g \rightarrow h}(z, Q^2)$ are the fragmentation functions in vacuum and the modification to the splitting functions,

$$\begin{aligned} \Delta\gamma_{q \rightarrow qg}(z, x_B, x_L, l_T^2) &= \frac{C_A}{l_T^2} \left[\frac{1+z^2}{(1-z)_+} T_{qg}^A(x_B, x_L) + \delta(1-z) \Delta^{(q)} T_{qg}^A(x_B, l_T^2) \right] \\ &\quad \times \frac{2\pi\alpha_s}{N_c f_q^A(x_B)} \\ \Delta\gamma_{q \rightarrow gq}(z, x_B, x_L, l_T^2) &= \Delta\gamma_{q \rightarrow qg}(1-z, x_B, x_L, l_T^2) \end{aligned} \quad (5)$$

are obtained from the induced gluon bremsstrahlung spectra and therefore are related to the twist-four nuclear quark-gluon correlation distribution,

$$\begin{aligned} T_{qg}^A(x_B, x_L) &= \int \frac{dy^-}{2\pi} dy_1^- dy_2^- e^{i(x_B+x_L)p^+y^-} (1 - e^{-ix_L p^+ y_2^-}) (1 - e^{-ix_L p^+ (y^- - y_1^-)}) \\ &\quad \times \frac{1}{2} \langle A | \bar{\psi}_q(0) \gamma^+ F_{\sigma^+}(y_2^-) F^{+\sigma}(y_1^-) \psi_q(y^-) | A \rangle \theta(-y_2^-) \theta(y^- - y_1^-). \end{aligned} \quad (6)$$

The matrix element,

$$\Delta^{(q)} T_{qg}^A(x, \ell_T^2) \equiv \int_0^1 dz \frac{1}{1-z} [2T_{qg}^A(x, x_L)|_{z=1} - (1+z^2)T_{qg}^A(x, x_L)], \quad (7)$$

in the second term (which is proportional to a $\delta(1-z)$ function) of the modification to the splitting function comes from virtual corrections to the multiple parton scattering cross section. This term can be constructed from the momentum sum rule (or momentum conservation) for the modified fragmentation function [6, 7, 37],

$$\int dz z \Delta D_q^h(z, Q^2) = 0. \quad (8)$$

The quark distribution function $f_q^A(x_B)$ of the nucleus is defined as

$$f_q^A(x_B) = \int \frac{dy^-}{2\pi} e^{ix_B p^+ y^-} \frac{1}{2} \langle A | \bar{\psi}_q(0) \gamma^+ \psi_q(y^-) | A \rangle. \quad (9)$$

With this modification to the fragmentation functions from single induced gluon emission, one can calculate the modified fragmentation functions by including the vacuum fragmentation functions which satisfy the vacuum DGLAP evolution equations,

$$\tilde{D}_q^h(z, Q^2) = D_q^h(z, Q^2) + \Delta D_q^h(z, Q^2). \quad (10)$$

If one defines the parton energy loss as the energy carried away by the radiated gluon, one obtains

$$\begin{aligned}\frac{\Delta E}{E} &= \langle \Delta z_g \rangle = \frac{\alpha_s}{2\pi} \int \frac{dl_T^2}{l_T^2} \int dz z \Delta \gamma_{q \rightarrow gq}(z, l_T^2) \\ &= \alpha_s^2 \int dl_T^2 \int_0^1 dz \frac{C_A}{N_c} \frac{1 + (1-z)^2}{l_T^4} \frac{T_{qg}^A(x_B, x_L)}{f_q^A(x_B)}.\end{aligned}\quad (11)$$

Assuming factorization of the two parton correlation distribution T_{qg}^A in terms of quark and gluon distributions in nucleons [40, 41], one can express the twist-four nuclear quark-gluon correlation distribution,

$$\begin{aligned}\frac{2\pi\alpha_s}{N_c} \frac{T_{qg}^A(x_B, x_L)}{f_q^A(x_B)} &= \frac{2\pi\alpha_s}{N_c} \pi \int dy^- \rho_N^A(y) [1 - \cos(x_L p^+ y^-)] \\ &\quad \times [(x_L G_N(x_L) + c(x_L) [x G_N(x)]_{x \approx 0})] \\ &= \int dy^- [1 - \cos(x_L p^+ y^-)] [\hat{q}_F(x_L, y) + c(x_L) \hat{q}_F(0, y)]\end{aligned}\quad (12)$$

in terms of the generalized jet transport parameter in nuclear medium,

$$\hat{q}_R(x_L, y) = \frac{4\pi^2 \alpha_s C_R}{N_c^2 - 1} \rho_N^A(y) x_L G_N(x_L), \quad (13)$$

which in the limit of $x_L = 0$ is also the transverse momentum broadening per unit distance for a parton in the R -representation of color. Here $c(x_L) = f_q^A(x_B + x_L)/f_q^A(x_B)$. The momentum fraction x_L dependence in the generalized transport parameter reflects the energy transfer to the medium parton during the inelastic scattering with the propagating parton. Such recoil of the medium parton is in fact the cause for elastic energy loss [42]. We will limit the study to gluon bremsstrahlung and therefore will not consider the x_L dependence of the generalized jet transport parameter $\hat{q}(x_L, y) \approx \hat{q}(0, y) \equiv \hat{q}(y)$. Under this approximation,

$$\frac{2\pi\alpha_s}{N_c} \frac{T_{qg}^A(x_B, x_L)}{f_q^A(x_B)} \approx \int dy^- \hat{q}_F(y) 4 \sin^2(x_L p^+ y^- / 2). \quad (14)$$

Since $x_L = \infty$ for $z = 0$ and both the quark $f_q^A(x_B + x_L)$ and gluon distributions $x_L G_N(x_L)$ vanish at $x_L = \infty$, the matrix elements related to the virtual correction in the modified fragmentation function becomes

$$\frac{2\pi\alpha_s}{N_c} \frac{\Delta^{(q)} T_{qg}^A(x, \ell_T^2)}{f_q^A(x_B)} \approx - \int_\epsilon^{1-\epsilon} dz \frac{1+z^2}{1-z} \int dy^- \hat{q}_F(y) 4 \sin^2(x_L p^+ y^- / 2), \quad (15)$$

where

$$\epsilon(l_T^2) = \frac{1}{2} \left(1 - \sqrt{1 - 2l_T^2/p^+ q^-} \right); \quad l_T^2 \leq 2p^+ q^- \quad (16)$$

are the restrictions imposed on the limits of z and l_T^2 integrations by requiring $x_L \leq 1$. Such limits are also imposed in the calculation of the modified fragmentation function. The radiated parton energy loss from single secondary scattering is then

$$\frac{\Delta E}{E} = C_A \frac{\alpha_s}{2\pi} \int dy^- \int_0^{Q^2} \frac{dl_T^2}{l_T^4} \int_\epsilon^{1-\epsilon} dz [1 + (1-z)^2] \hat{q}_F(y) 4 \sin^2(x_L p^+ y^- / 2). \quad (17)$$

III. MODIFIED DGLAP EVOLUTION EQUATIONS

To take into account of multiple induced gluon emissions, one can follow the resummation of gluon bremsstrahlung in vacuum and assume that multiple medium induced bremsstrahlung can be resummed in the same way and one can

obtain the mDGLAP evolution equations for the modified fragmentation functions [6, 7],

$$\frac{\partial \tilde{D}_q^h(z_h, \mu^2)}{\partial \ln \mu^2} = \frac{\alpha_s(\mu^2)}{2\pi} \int_{z_h}^1 \frac{dz}{z} \left[\tilde{\gamma}_{q \rightarrow qg}(z, \mu^2) \tilde{D}_q^h\left(\frac{z_h}{z}, \mu^2\right) + \tilde{\gamma}_{q \rightarrow gq}(z, \mu^2) \tilde{D}_g^h\left(\frac{z_h}{z}, \mu^2\right) \right], \quad (18)$$

$$\frac{\partial \tilde{D}_g^h(z_h, \mu^2)}{\partial \ln \mu^2} = \frac{\alpha_s(\mu^2)}{2\pi} \int_{z_h}^1 \frac{dz}{z} \left[\sum_{q=1}^{2n_f} \tilde{\gamma}_{g \rightarrow q\bar{q}}(z, \mu^2) \tilde{D}_q^h\left(\frac{z_h}{z}, \mu^2\right) + \tilde{\gamma}_{g \rightarrow gg}(z, \mu^2) \tilde{D}_g^h\left(\frac{z_h}{z}, \mu^2\right) \right], \quad (19)$$

where the modified splitting functions are given by the sum of the vacuum ones $\gamma_{a \rightarrow bc}(z)$ and the medium modification $\Delta\gamma_{a \rightarrow bc}(z, l_T^2)$,

$$\tilde{\gamma}_{a \rightarrow bc}(z, l_T^2) = \gamma_{a \rightarrow bc}(z) + \Delta\gamma_{a \rightarrow bc}(z, l_T^2) \quad (20)$$

with $\Delta\gamma_{a \rightarrow bc}(z, l_T^2)$ for $q \rightarrow qg$ given in Eq. (5). In the above mDGLAP evolution equations we deliberately used μ^2 to denote the evolving scale whose maximum value in DIS is Q^2

In addition to the first mDGLAP evolution equation for the modified quark fragmentation function in Eq. (18) as derived in Refs. [6, 7] in DIS off nuclei, one has to consider multiple scattering and induced gluon bremsstrahlung for a gluon jet in order to complete the mDGLAP evolution equation for medium modified gluon fragmentation function in Eq. (19) and the corresponding modified splitting functions. In the study of contributions from quark-quark (antiquark) double scattering to the modified quark fragmentation functions within the same framework of generalized factorization of multiple parton scattering [43], one can in fact relate the effective splitting functions to the corresponding parton-parton scattering amplitudes. From gluon-gluon scattering matrix elements, one can obtain the following medium modification to the splitting functions (see Appendix 3 in Ref. [43]) due to double scattering between a gluon jet and medium gluons,

$$\Delta\gamma_{g \rightarrow q\bar{q}}(z, l_T^2) = \frac{1}{2l_T^2} [z^2 + (1-z)^2] \left[1 - \frac{N_c}{C_F} z(1-z) \right] \times \int dy^- \hat{q}_F(y) 4 \sin^2(x_L p^+ y^- / 2) \quad (21)$$

$$\Delta\gamma_{g \rightarrow gg}(z, l_T^2) = \frac{2C_A N_c}{l_T^2 C_F} \frac{(1-z+z^2)^3}{z(1-z)_+} \int dy^- \hat{q}_F(y) 4 \sin^2(x_L p^+ y^- / 2) - \delta(1-z) \frac{\Delta_g(l_T^2)}{l_T^2}; \quad (22)$$

$$\Delta_g(l_T^2) = \int dy^- \int_{\epsilon}^{1-\epsilon} dz \left\{ n_f [z^2 + (1-z)^2] \left[1 - \frac{N_c}{C_F} z(1-z) \right] + \frac{2C_A N_c}{C_F} \frac{(1-z+z^2)^3}{z(1-z)} \right\} \hat{q}_F(y) 4 \sin^2(x_L p^+ y^- / 2), \quad (23)$$

where we have similarly assumed that the parton correlation distribution vanishes for $x_L \geq 1$ which imposes limit on the integration over $\epsilon(l_T^2) \leq z \leq 1 - \epsilon(l_T^2)$. The above calculations of the modification to the splitting functions are more complete since they include non-leading terms when $1-z \rightarrow 0$. For mDGLAP evolution equation for the quark fragmentation function, one can also compute the modification to the splitting function for $q \rightarrow qg$ from the complete matrix element of quark-gluon Compton scattering ((see Appendix 3 in Ref. [43]),

$$\Delta\gamma_{q \rightarrow qg}(z, l_T^2) = \frac{1}{l_T^2} \left[C_A \frac{z(1+z^2)}{(1-z)_+} + C_F(1-z)(1+z^2) \right] \times \int dy^- \hat{q}_F(y) 4 \sin^2(x_L p^+ y^- / 2) - \delta(1-z) \frac{\Delta_q(l_T^2)}{l_T^2}; \quad (24)$$

$$\Delta_q(l_T^2) = \int dy^- \int_{\epsilon}^{1-\epsilon} dz \left[C_A \frac{z(1+z^2)}{1-z} + C_F(1-z)(1+z^2) \right] \times \hat{q}_F(y) 4 \sin^2(x_L p^+ y^- / 2). \quad (25)$$

Note that we have expressed the medium modifications to the splitting functions in mDGLAP evolution equations for both quark and gluon fragmentation functions in terms of the quark jet transport parameter \hat{q}_F and leave the color factors explicitly in the z -dependent parts. There is no single overall color factor for each effective splitting functions because they involve more than one channel of quark-gluon or gluon-gluon scattering which have different color factors. However, in the limit of soft gluon radiation, $z \rightarrow 1$ (here z is the momentum fraction carried by the leading parton), the modifications are dominated by leading term $1/(1-z)$. In this case,

$$\Delta\gamma_{g \rightarrow gg}(z, l_T^2) \approx \frac{N_c}{C_F} \Delta\gamma_{q \rightarrow qg}(z, l_T^2), \quad \text{for } z \rightarrow 1, \quad (26)$$

and $N_c/C_F = 2N_c^2/(N_c^2 - 1) = 9/4$.

We can also similarly consider the quark-quark (antiquark) scattering and quark-antiquark annihilation processes for the secondary scattering. These processes will be responsible for flavor changing (conversion) in the parton propagation. They generally involve quark or antiquark density distributions of the medium and are also suppressed by a factor of l_T^2/Q^2 [43]. We will neglect these processes for now and focus on the most dominant gluon radiation in the mDGLAP equations.

In the following we will numerically solve the mDGLAP evolution equations for the modified fragmentation functions using a modified HOPPET (Higher Order Perturbative Parton Evolution Toolkit) [44] in LO. HOPPET is a Fortran95 package with the GNU Public License that carries out the vacuum DGLAP evolution in z -space using Runge-Kutta method with a given initial condition $D_a(z, Q_0^2)$. We replace the normal LO splitting functions in HOPPET with the modified splitting functions in each step of Runge-Kutta iteration to solve the mDGLAP evolution for modified fragmentation functions.

Since all the medium modified splitting functions in mDGLAP evolution equations are proportional to the path integral of the jet transport parameter $\hat{q}_F(y)$ along the parton propagation length, the modified fragmentation functions will be determined completely by the spatial profile (and time evolution in the case of heavy-ion collisions) of the $\hat{q}_F(y)$ which characterizes the properties of the medium that a jet probes. Therefore, we will study in the rest of this paper the dependence of the modified fragmentation functions on the profile of the jet transport parameter, its value, length of the medium, in addition to the energy (E) and scale (Q^2) dependence. By setting $\hat{q}_F(y) = 0$, the mDGLAP evolution equations will become those in vacuum and the corresponding vacuum fragmentation functions and their Q^2 dependence will be recovered.

IV. THE ‘‘BRICK’’ PROBLEM

We will consider first the simplest profile of the medium characterized by a constant value of $\hat{q}_F = \hat{q}_0$ for a uniform medium with finite length L , assuming that a jet is produced at $y = 0$ via DIS and propagates through the medium and finally hadronizes outside the medium. Such a ‘‘brick’’ problem is illustrative for understanding the main features of the modified fragmentation function from mDGLAP evolution equations. When solving mDGLAP evolution equations in this paper, we will use their LO form with $n_f = 3$ number of quark flavors and a running strong coupling constant $\alpha_s(Q^2)$ with $\Lambda_{\text{QCD}} = 214$ MeV.

A. Initial conditions

To solve the mDGLAP evolution equations one also has to specify the fragmentation functions at an initial scale Q_0^2 as the initial condition. Such initial conditions in principle should be different in medium and vacuum. Since perturbative QCD cannot be applied below the initial scale Q_0^2 the initial conditions are normally supplied by experimental measurements which are currently not available for medium modified fragmentation functions. Without such information, we will have to resort to a model of the medium modified fragmentation function at the initial scale Q_0^2 . Many studies [34, 36] with the modified DGLAP evolution approach have simply assumed the initial condition at Q_0^2 in medium as the same in vacuum. This implies that partons below scale Q_0^2 will not interact with the medium and therefore suffer no energy loss. This is apparently counterintuitive in theory. Phenomenologically, such an assumption also means that all medium modification comes from processes above scale Q_0^2 and therefore has a very strong Q^2 dependence, which contradicts the experimental data as we will see later. To take into account medium modification to the fragmentation functions below the initial scale Q_0^2 , we will assume in this study,

$$\tilde{D}_a(Q_0^2) = D_a(Q_0^2) + \Delta D_a(Q_0^2), \quad a = g, q, \bar{q}. \quad (27)$$

where $D_a(Q_0^2)$ is the vacuum fragmentation function and $\Delta D_a(Q_0^2)$ will be generated purely from medium via the mDGLAP equations (18) starting at $\mu^2 = 0$. In practice, we will simply set the effective splitting functions to contain

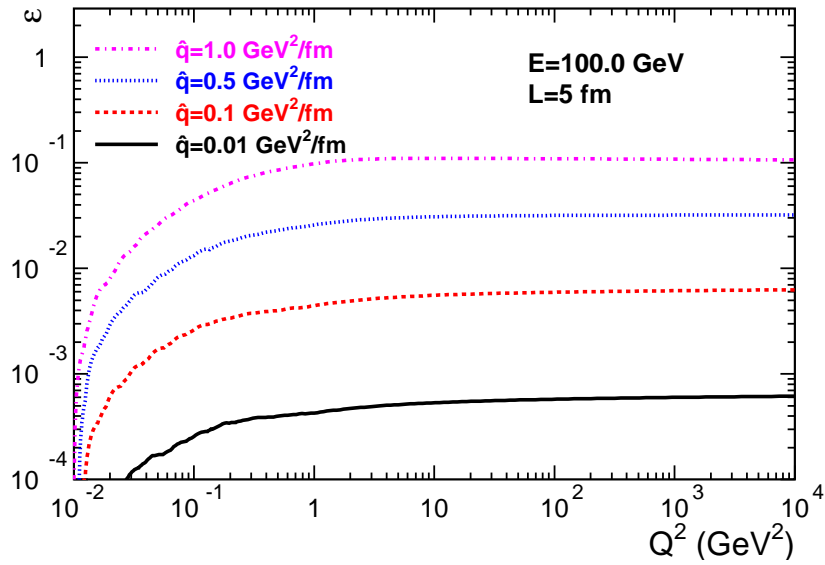


FIG. 2: (color online) Numerical violation of the momentum sum rule for the fragmentation function of a u quark as a function of the momentum scale Q^2 and for different values of the jet transport parameter \hat{q}_0 .

only the medium-induced parts, $\tilde{\gamma}_{a \rightarrow bc}(z, l_T^2) = \Delta\gamma_{a \rightarrow bc}(z, l_T^2)$, freeze the running strong coupling constant at $\mu^2 = Q_0^2$ and use the vacuum fragmentation functions as initial condition at $\mu^2 = 0$ in the calculation of $\Delta D_a(Q_0^2)$. The value of Q_0^2 will be set at $Q_0^2 = 1 \text{ GeV}^2$ in this study unless otherwise stated.

B. Momentum sum rule

To test the modified HOPPET method and estimate errors of the numerical solution to the mDGLAP evolution equations, we first check the following momentum sum rules

$$\sum_h \int_0^1 dz z \tilde{D}_a^h(z, Q^2) = 1, \quad (28)$$

which should be satisfied for all parton fragmentation functions at any scale Q^2 . For this test, we assume the following initial fragmentation functions,

$$D_q^h(z, Q_0^2) = D_{\bar{q}}^h(z, Q_0^2) = D_g^h(z, Q_0^2) = \delta(1 - z). \quad (29)$$

which corresponds to a parton-hadron duality in vacuum at scale Q_0^2 with just one hadron species. Medium modification of the initial condition at Q_0^2 will be given according to the prescription in Sec. IV A.

Shown in Fig. 2, is the numerical violation of the above momentum sum rule for u quark fragmentation functions

$$\varepsilon = 1 - \int_0^1 dz z \tilde{D}_u^h(z, Q^2), \quad (30)$$

in medium with different values of jet transport parameter \hat{q}_0 . The sum rule for the fragmentation function in vacuum ($\hat{q}_0 = 0$) is almost perfect and is also the case for small values of jet transport parameter $\hat{q}_0 \leq 0.1 \text{ GeV}^2/\text{fm}$. The numerical error becomes larger as the value of \hat{q}_0 is increased in the “brick” medium. The HOPPET method uses a grid in z -space to numerically evaluate integration in z . This grid in z has a minimum value z_{min} . Therefore the numerical integration over z is always truncated in z space below z_{min} . Even though $z_{min} = e^{-30}$ in this study is a very small number but not exactly zero. So, the momentum fraction contained in the $z < z_{min}$ region causes the numerical violation of the momentum sum rule. Such violation should increase with Q^2 and \hat{q}_0 because the mDGLAP evolution puts more hadrons (or partons) in the small $z < z_{min}$ region at larger Q^2 or for larger values of \hat{q}_0 . However, the sum rules in medium are still satisfied with an error better than 10 percent for most of the range of Q^2 and \hat{q}_0 as shown in Fig. 2.

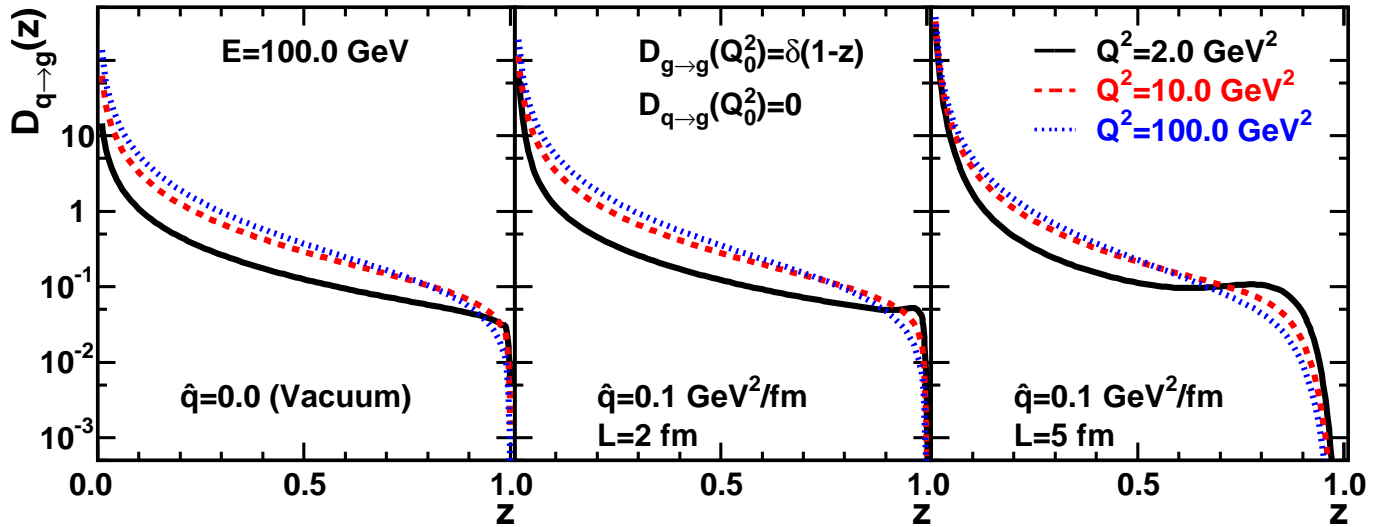


FIG. 3: (color online) Gluon distribution in the parton shower of a quark jet

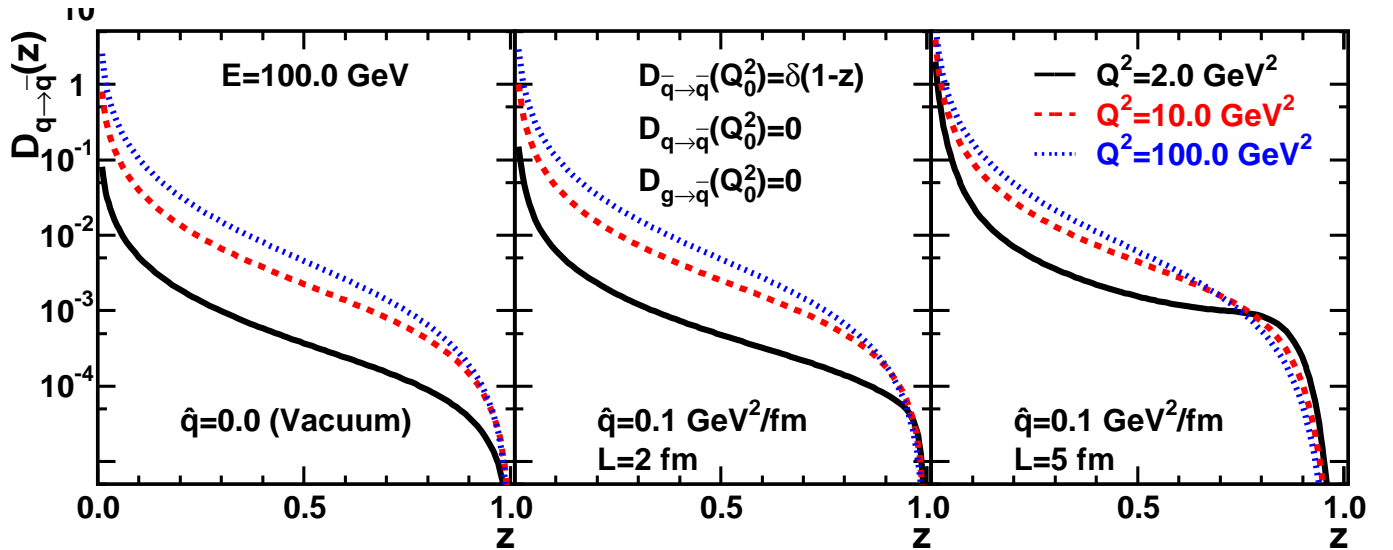


FIG. 4: (color online) Sea quark distribution in the parton shower of a quark jet

C. Shower parton distributions and energy loss

Before we turn our attention to the medium modified fragmentation functions, it is useful to study the shower parton distributions generated by a propagating parton which can provide useful information about the underlying parton production and energy loss before the final hadronization outside the medium. To this end, we again assume parton-hadron duality for three species of “hadrons”, $h = q, \bar{q}, g$ and take initial conditions,

$$D_a^a(z, Q_0^2) = \delta(1-z); D_a^{b \neq a}(z, Q_0^2) = 0 \quad (a, b = q, \bar{q}, g),$$

which simply mean that partons stop branching in vacuum at scale Q_0^2 . A parton with a large scale $Q^2 > Q_0^2$, however, will undergo both vacuum and medium induced gluon bremsstrahlung and pair production as described by the mDGLAP evolution equations in Eqs. (18) and (19). The original parton will then generate other species of partons within its parton shower. The initial condition for medium modification will be given by the prescription in Sec. IV A, which implies that jet-medium interaction continues to generate parton shower below scale Q_0^2 .

Shown in Figs. 3 and 4 are gluon $\tilde{D}_q^g(z, Q^2)$ and antiquark (or sea quark) distribution $\tilde{D}_q^{\bar{q}}(z, Q^2)$ within a quark jet for different values of jet transport parameter \hat{q}_0 , medium length L and momentum scale Q^2 . We have set $Q_0^2 = 1 \text{ GeV}^2$ and initial parton energy $E = 100 \text{ GeV}$. Yields of gluons and sea quarks within a quark jet increase with

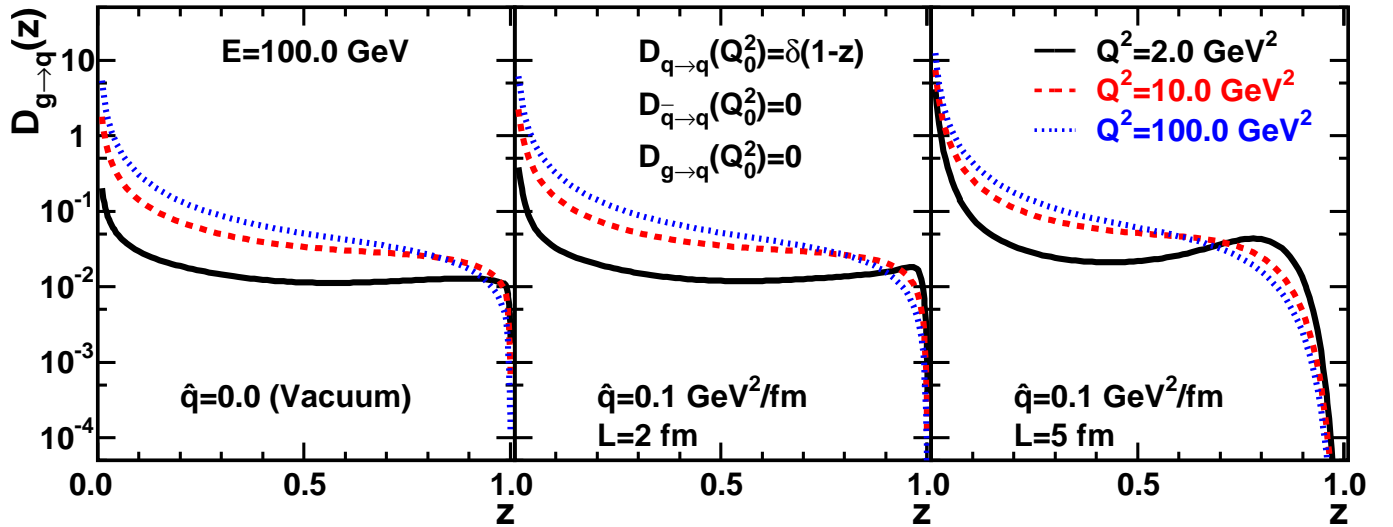


FIG. 5: (color online) Quark (antiquark) distribution in the parton shower of a gluon jet

Q^2 for both vacuum (left panels) and medium modified (middle and right panels) fragmentation functions and the spectra also soften as more gluon bremsstrahlung and pair production take place during the evolution with Q^2 . For small Q^2 the modified shower parton distributions become harder at large z due to medium-induced pair production of quark-anti-quark and gluons (in the $g \rightarrow g\bar{q}q$ splitting). However, with increasing Q^2 the modified fragmentation functions again soften and the yields increase with \hat{q}_0 and L due to the additional gluon bremsstrahlung and pair production induced by jet quenching during the propagation of the quark jet in medium. The sea quark distributions are generally softer than gluon distributions within a quark jet because quark-antiquark pairs are produced through gluon fission in vacuum and fusion in medium.

Similar behavior is also seen in quark(antiquark) distribution $\tilde{D}_g^q(z, Q^2)$ within a gluon jet as shown in Fig. 5. For small $Q^2 = 2 \text{ GeV}^2$, one notes that the distribution is quite flat, reflecting the shape of the splitting function $\tilde{\gamma}_{g \rightarrow q\bar{q}}(z)$ when the distribution is dominated by pair creation from the leading gluon whose initial distribution is peaked at $z = 1$. As one increases \hat{q}_0 , Q^2 and L , soft gluons are also generated which in turn produce soft quark-antiquark pairs. As a consequence, the final quark distribution within a gluon jet will become softer as the gluon distribution $\tilde{D}_g^g(z, Q^2)$ and sea quark distribution $\tilde{D}_q^{\bar{q}}(z, Q^2)$ within a quark jet in Figs. 3 and 4. The gluon distribution within a gluon jet on another hand contains both the initial gluon and produced gluons from vacuum and medium induced bremsstrahlung. As one can see from Fig. 6, it indeed develops a peak at $z \sim 0$ due to vacuum and induced bremsstrahlung in addition to the peak at $z = 1$ of its initial distribution as one increases the values of \hat{q}_0 , L and Q^2 . Since one cannot separate initial and produced gluons, the concept of parton energy loss becomes ambiguous for a gluon jet in this picture of successive bremsstrahlung in medium.

The case for a quark jet is different because net quark number is a conserved quantity. Even though the quark distribution contains both the initial leading or valence quark and the sea quarks from pair production, the sea quark distribution should be the same as the antiquark distribution and therefore can be subtracted. For the purpose of studying attenuation of the leading or valence parton due to vacuum and medium induced gluon bremsstrahlung we define the valence quark distribution as

$$\tilde{D}_q^v(z, Q^2) \equiv \tilde{D}_q^q(z, Q^2) - \tilde{D}_q^{\bar{q}}(z, Q^2). \quad (31)$$

Shown in Fig. 7 is the valence quark distribution from the mDGLAP evolution equations. Because of gluon bremsstrahlung and pair production during its evolution and propagation, the leading or valence quark distribution in both vacuum (left panel) and medium (middle and right panel) gradually softens from its initial $\delta(1-z)$ form as one increases the momentum scale Q^2 . Like other fragmentation functions, significant change of the valence quark distribution occurs already due to vacuum gluon bremsstrahlung and pair production when it evolves from the initial Q_0^2 . As one increases jet quenching parameter \hat{q}_0 and the medium length L , the valence quark distribution further softens.

Such softening of the valence quark distribution can be characterized by the total fractional momentum change

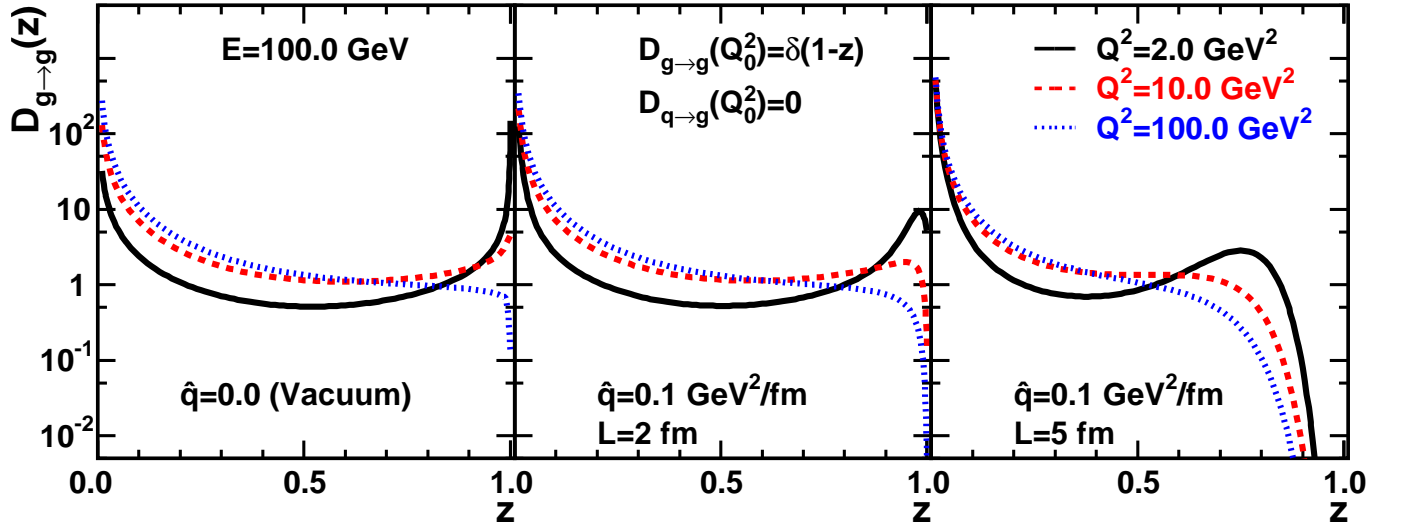


FIG. 6: (color online) Gluon distribution in the parton shower of a gluon jet.

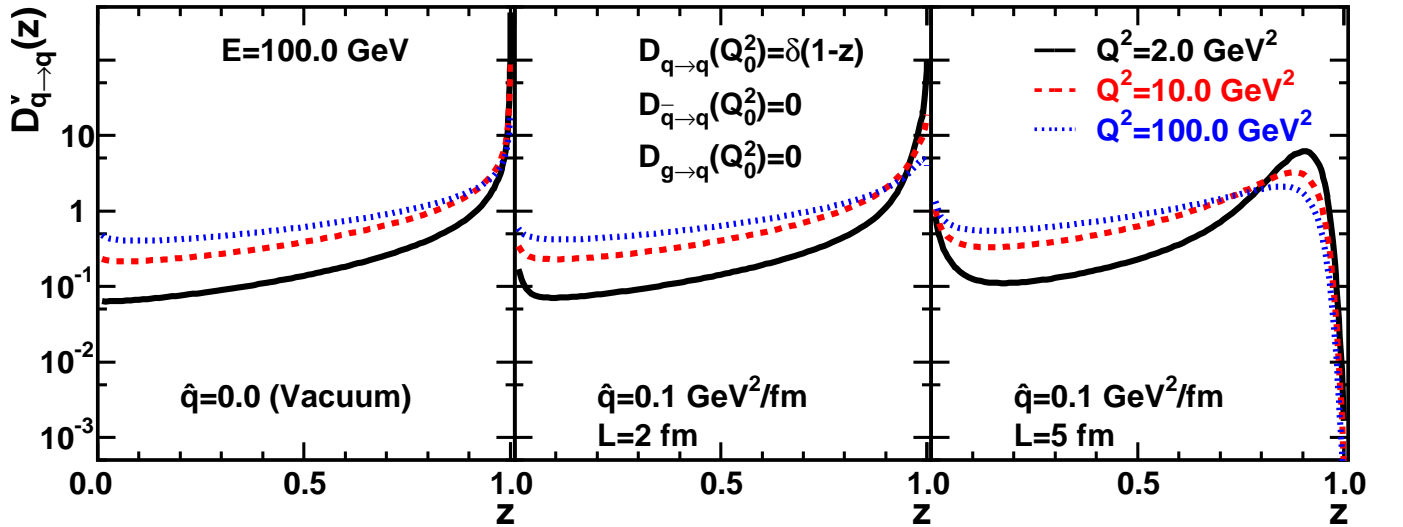


FIG. 7: (color online) Valence quark distribution in the parton shower of a quark jet

afforded by the valence quark for both vacuum and medium modified fragmentation functions

$$\frac{\Delta E_v}{E} = 1 - \int_0^1 dz z D_q^v(z, Q^2); \quad (32)$$

$$\frac{\Delta E_m}{E} = 1 - \int_0^1 dz z \tilde{D}_q^v(z, Q^2). \quad (33)$$

The net energy loss due to medium induced gluon bremsstrahlung and pair production is then

$$\frac{\Delta E}{E} = \frac{\Delta E_m - \Delta E_v}{E} = \int_0^1 dz z \left[D_q^v(z, Q^2) - \tilde{D}_q^v(z, Q^2) \right]. \quad (34)$$

Shown in Fig. (8) is the medium induced energy loss as a function of the medium length L and initial jet energy E for different values of \hat{q}_0 . Because of non-Abelian LPM interference, parton energy loss induced by multiple scattering as seen in the left panel clearly shows a quadratic dependence on the medium length [3]. However, for fixed initial parton energy E and jet transport parameter \hat{q}_0 , such quadratic length dependence gives away to a linear dependence for large values of medium length and the induced energy loss even saturates as $\Delta E/E$ approaches to 1 because energy conservation imposed on each step of the mDGLAP evolution.

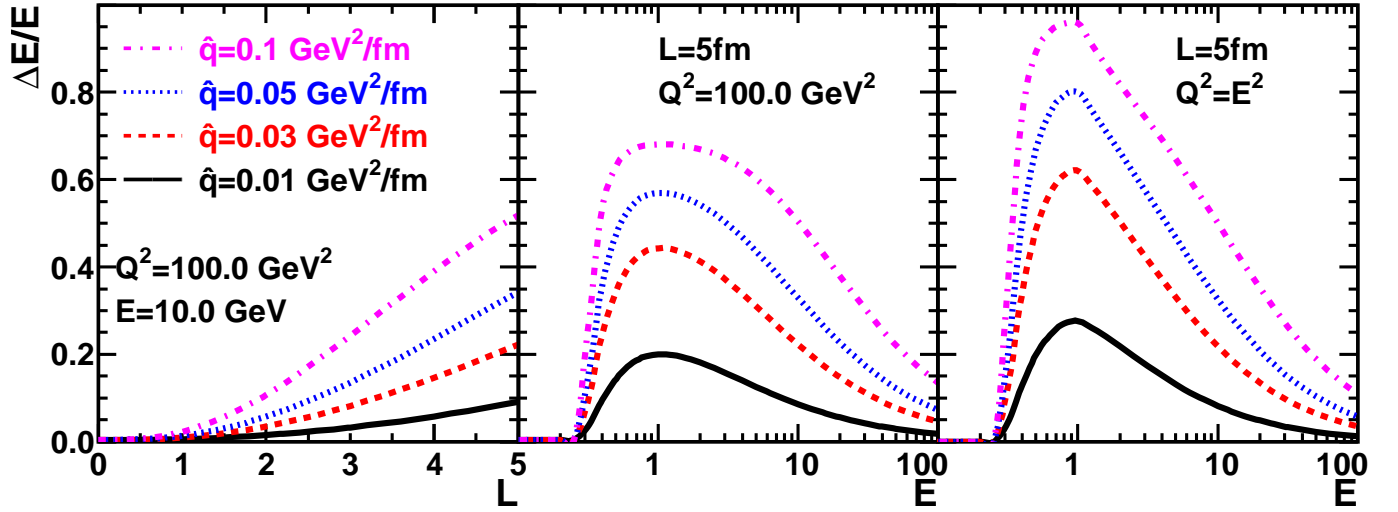


FIG. 8: (color online) Energy and length dependence of medium induced energy loss of a valence quark from mDGLAP evolution.

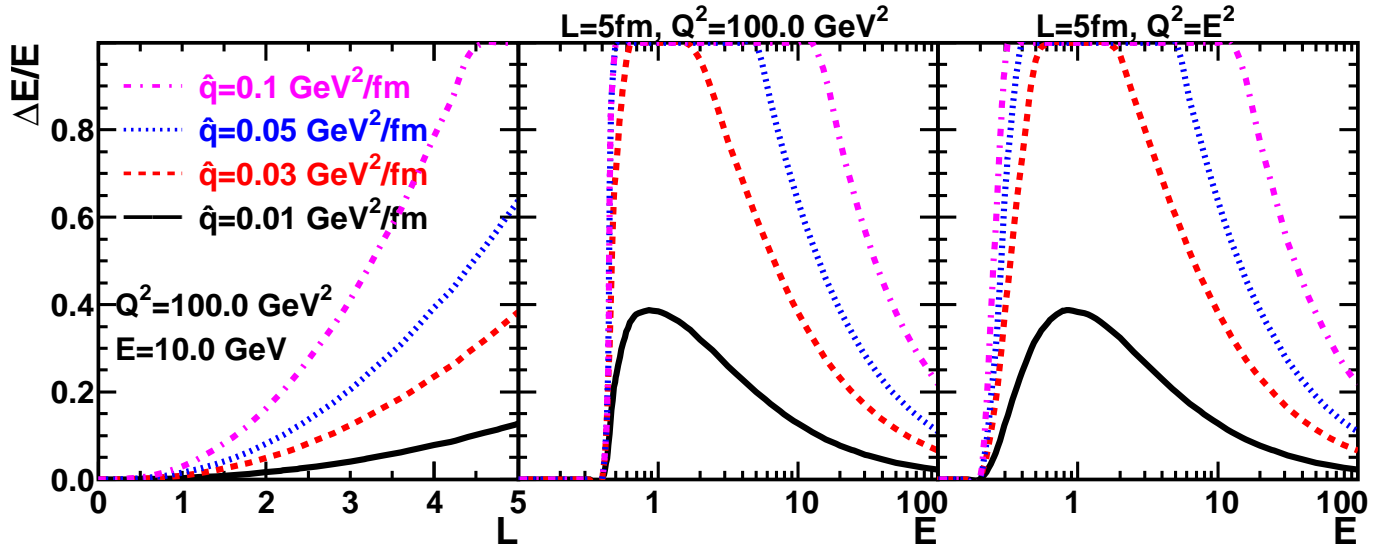


FIG. 9: (color online) Energy and length dependence of radiated energy loss of a quark from single gluon bremsstrahlung induced by multiple scattering.

The behavior of such parton energy loss as defined by Eq. (34) with the modified fragmentation functions from mDGLAP evolution is quantitatively and sometime qualitatively different from the averaged radiative energy loss via a single gluon emission induced by multiple scattering. The averaged energy loss via single gluon emission is usually identified with the energy carried by the radiated gluon [Eq. (17)] as shown in Fig. 9. Even though energy and momentum is conserved in the gluon bremsstrahlung process as described by the higher-twist formalism, energy loss in this case of single gluon emission involves energy loss per emission multiplied by the average number of scatterings which could become a large number. Such a calculation apparently becomes invalid when $\Delta E/E \geq 1$. This is an indication of the need for resummation in terms of mDGLAP evolution in which unitarity of multiple emission is ensured.

In the calculation of energy loss in both the single gluon emission and the evolution of mDGLAP equations, we have imposed kinematic cut-off [Eq. (16)] for the integration over fractional longitudinal and transverse momentum. This is the reason for the strong energy dependence of the energy loss for small values of E . The asymptotic energy dependence of the energy loss ΔE in both cases is weaker than linear though the results from mDGLAP evolution shows weaker E dependence than the single gluon emission.

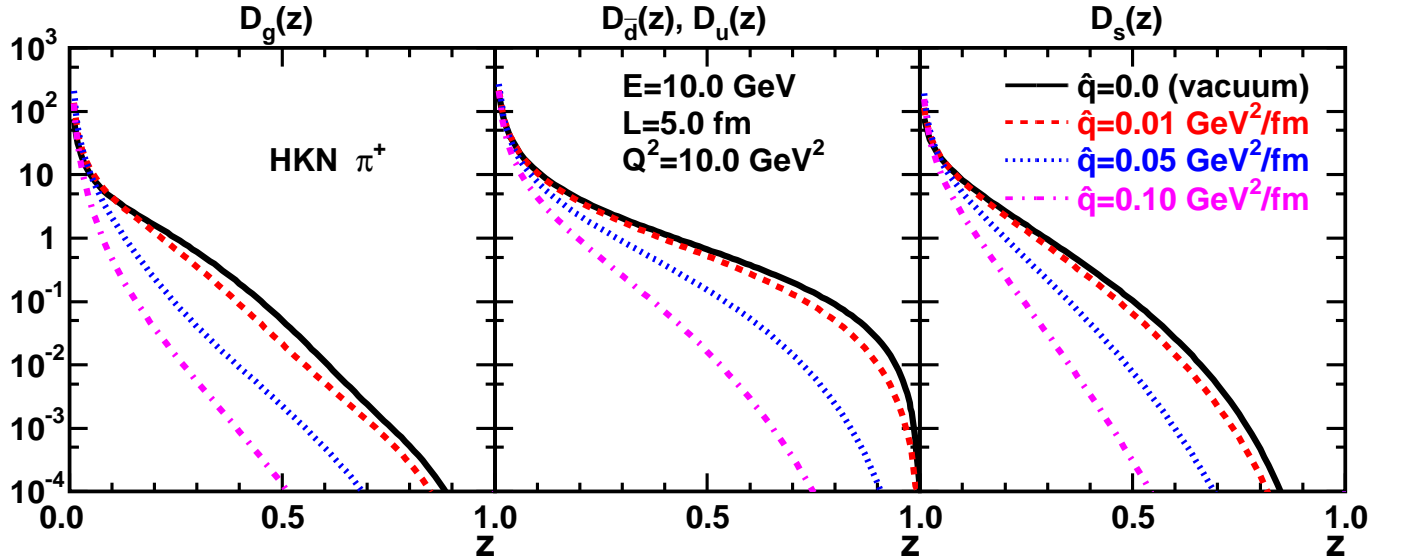


FIG. 10: (color online) Modified π fragmentation function of a gluon (right), up, down (middle) and strange (left) quark jet that is produced at momentum scale $Q^2 = 10 \text{ GeV}^2$ with initial energy $E = 10 \text{ GeV}$ and propagates through a uniform medium with length $L = 5 \text{ fm}$ and jet transport parameter $\hat{q}_0 = 0$ (vacuum fragmentation function) (solid), 0.01 (dashed), 0.05 (dotted) and 0.1 GeV^2/fm (dot-dashed). The initial condition to the mDGLAP evolution at Q_0^2 is given by HKN [50] parameterization

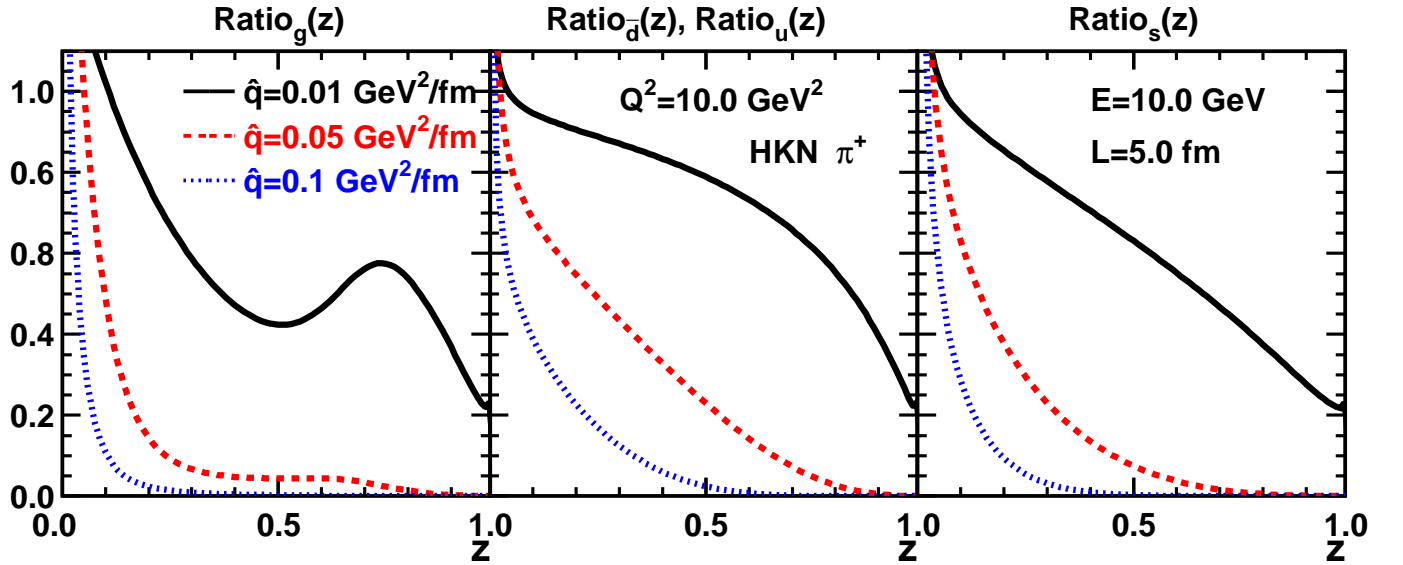


FIG. 11: (color online) The modification factor $R_a^\pi(z, Q^2)$ for the medium modified fragmentation function in Fig. 10.

D. Modified Fragmentation Functions

In the following, we will solve mDGLAP evolution equations with the initial conditions $D_a^h(z, Q_0^2)$ given by the HKN [50] parameterization of experimental measurements of fragmentation functions at $Q_0^2 = 1 \text{ GeV}^2$ and obtain the corresponding medium modified fragmentation functions for hadron production. To quantify the medium modification of the fragmentation functions, we define the modification factor

$$R_a^h(z, Q^2) = \frac{\tilde{D}_a^h(z, Q^2)}{D_a^h(z, Q^2)}, \quad (35)$$

as the ratio between modified and vacuum fragmentation functions.

Shown in Figs. 10 and 11 are the modified π^+ fragmentation functions for gluon (left panel), u , \bar{d} (middle panel) and

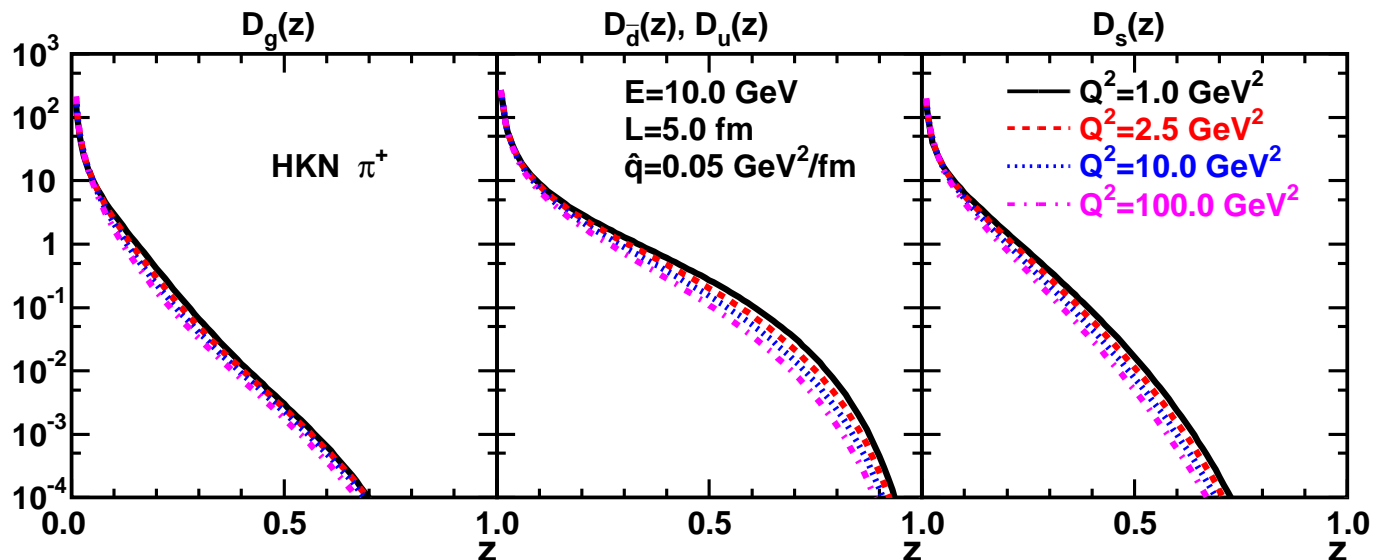


FIG. 12: (color online) Modified π fragmentation function of a gluon (right), up, down (middle) and strange (left) quark jet with initial energy $E = 10$ GeV that propagates through a uniform medium with length $L = 5$ fm and jet transport parameter $\hat{q}_0 = 0.05$ GeV²/fm. The momentum scale of jet production is $Q^2 = 1.0$ (solid), 2.5 (dashed), 10 GeV² (dotted) and 100 GeV (dot-dashed).

s (left panel) quark jets and the corresponding modification factors, respectively, for different values of jet transport parameter \hat{q}_0 in a uniform medium with length $L = 5$ fm. The initial jet energy is set to $E = 10$ GeV with virtuality $Q^2 = 10$ GeV². The modified fragmentation functions are seen to be suppressed at medium and large momentum fraction z with increasing values of \hat{q}_0 because of increased induced gluon bremsstrahlung and pair production. The produced soft gluons and sea quarks will also hadronize and contribute to the hadron spectra, leading to enhancement of medium modified fragmentation functions at small z . Since the medium modified gluon splitting function is about $9/4$ of a quark [Eq. (26)] at large z , it radiates more soft gluons and consequently its modified fragmentation is more suppressed at intermedium and large z as compared to the quark fragmentation functions.

At large z , the modification factor for gluon jets is seen to have a small bump for small values of \hat{q} . This feature results from the competition between gluon bremsstrahlung and pair production in the evolution of a gluon jet. Both of two processes contribute to the vacuum evolution. In the medium, however, gluon bremsstrahlung suppresses the fragmentation function while pair production is relatively enhanced in particular at large z . If one switches off the medium induced $g \rightarrow gg$ and $g \rightarrow q\bar{q}$ channels, the bump disappears. This feature is similar to the shower parton distributions of a gluon jet as discussed in the last subsection. However, as one increases the value of \hat{q} , these features at large z disappear as induced gluon bremsstrahlung further suppresses the gluon fragmentation functions.

Since the modification to the effective splitting functions due to gluon bremsstrahlung induced by multiple scattering are power suppressed at large Q^2 , most of the the modification to the fragmentation functions should come from mDGLAP evolution at small Q^2 . Shown in Figs. 12 and 13 are the modified fragmentation functions and the corresponding modification factors for different Q^2 but for fixed initial energy E and value of $\hat{q}_0 = 0.05$ GeV²/fm. The fragmentation functions at $Q_0^2 = 1$ GeV² correspond to the medium modified initial conditions that we generate according to our assumed prescription in this paper. One can see in Fig. 13 that the initial fragmentation functions are already suppressed at large z due to induced gluon emission and therefore most of the modification comes from mDGLAP evolution near or below the initial value of $Q^2 = Q_0^2$. Medium modification above the initial scale is relatively small. This will give a weak Q^2 dependence of the medium modification of the fragmentation functions as we will show in the discussion of jet quenching in DIS. The modification, however, varies with the initial energy E significantly, as shown in Figs. 14 and 15 for a fixed value of $\hat{q}_0 = 0.05$ GeV²/fm. Such variations reflect the energy dependence of the energy loss as shown in Fig. 8. Eventually, when the initial energy becomes infinitely large, the modification will become increasingly smaller.

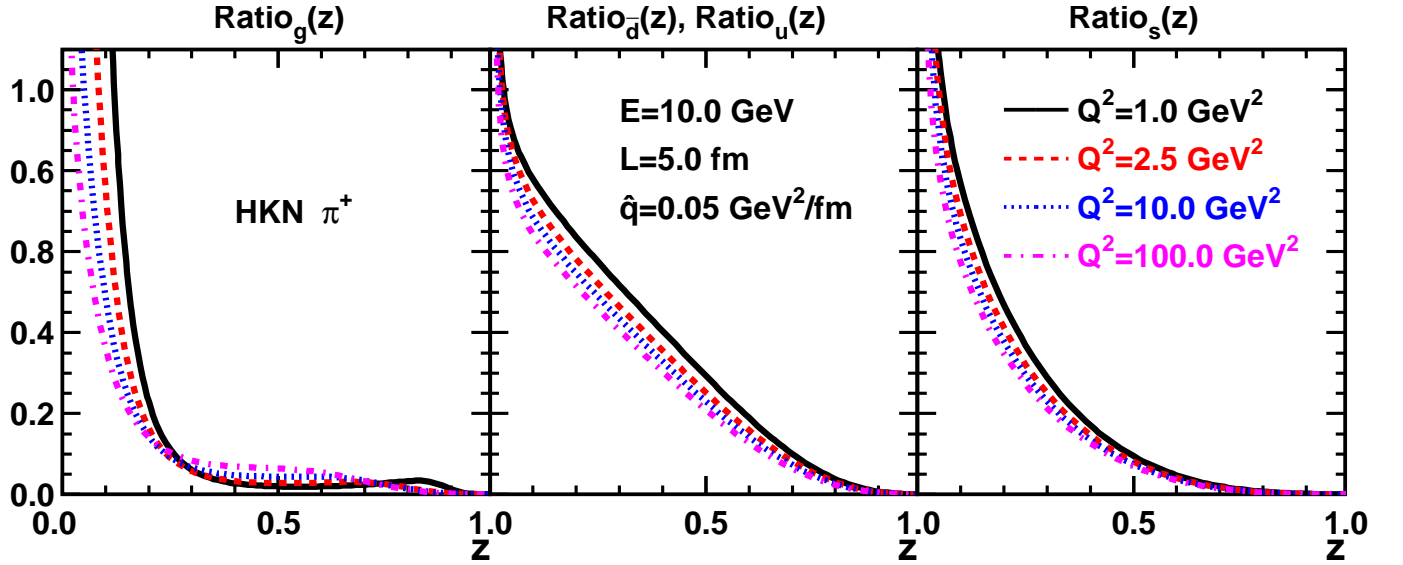


FIG. 13: (color online) The modification factor $R_a^\pi(z, Q^2)$ for the medium modified fragmentation function in Fig. 12.

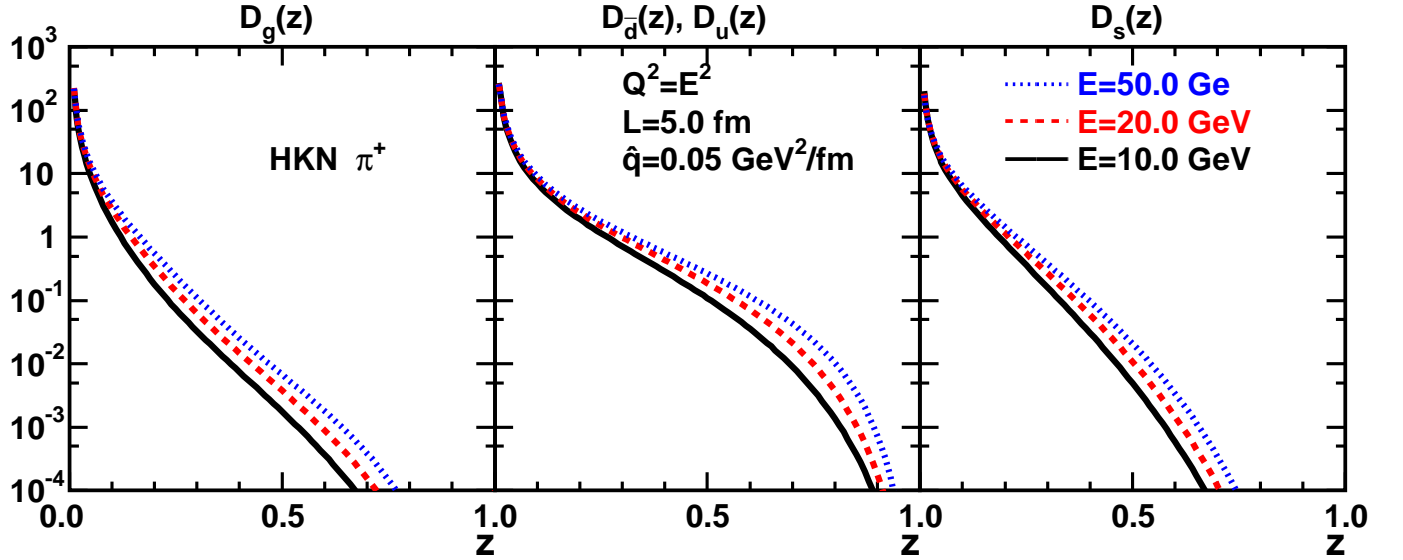


FIG. 14: (color online) Modified π fragmentation function of a gluon (right), up, down (middle) and strange (left) quark jet with initial energy $E = 10$ (solid), 20 (dashed) and 50 GeV (dotted) that propagates through a uniform medium with length $L = 5$ fm and jet transport parameter $\hat{q}_0 = 0.05$ GeV²/fm. The momentum scale of jet production is $Q^2 = E^2$.

V. MODIFIED FRAGMENTATION FUNCTIONS IN DIS

To calculate the nuclear modified fragmentation functions in semi-inclusive DIS off a nucleus we have to employ a more realistic form of the nuclear density distribution. We consider the initial quark jet produced at y_0 that travels along a direction with impact parameter b (see Fig. 16 for illustration). We assume that the jet transport parameter along the quark jet trajectory is proportional to the nuclear density,

$$\hat{q}(y, b) = \hat{q}_0 \frac{\rho_A(y, b)}{\rho_A(0, 0)}, \quad (36)$$

where $\rho_A(y, b)$ is the nuclear density distribution normalized as $\int dy d^2b \rho_A(y, b) = A$ and \hat{q}_0 is defined to be the jet transport parameter at the center of the nucleus. We will use the three-parameter Wood-Saxon form of nuclear density distribution here.

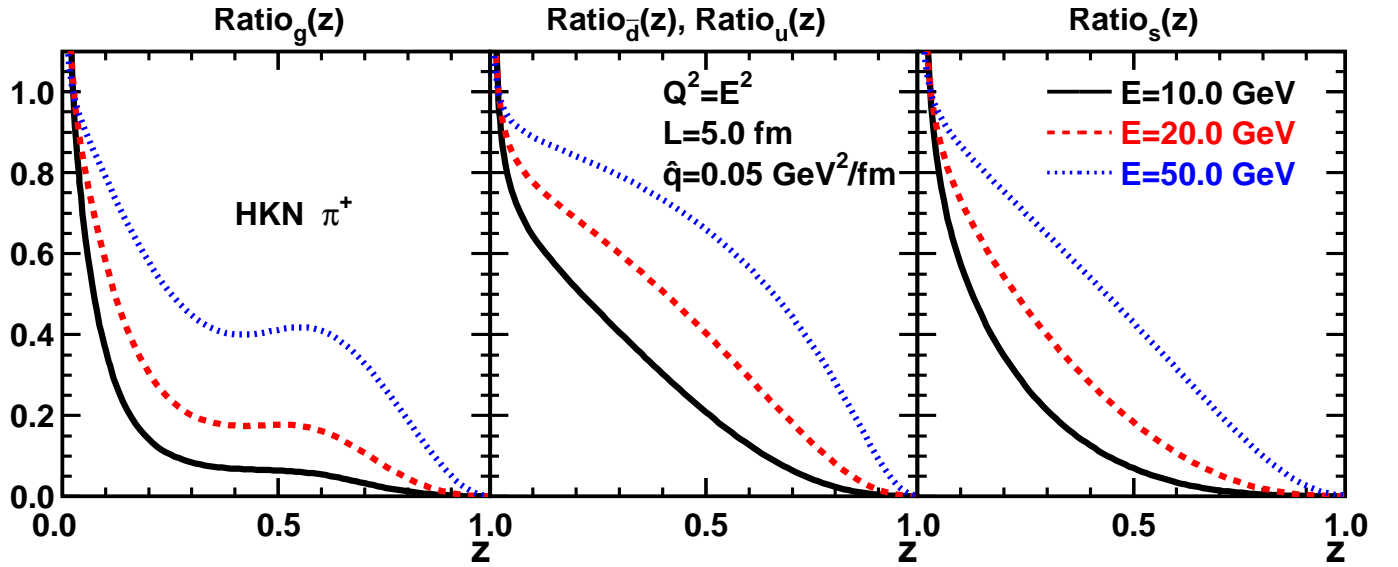


FIG. 15: (color online) The modification factor $R_a^\pi(z, Q^2)$ for the medium modified fragmentation function in Fig. 14.

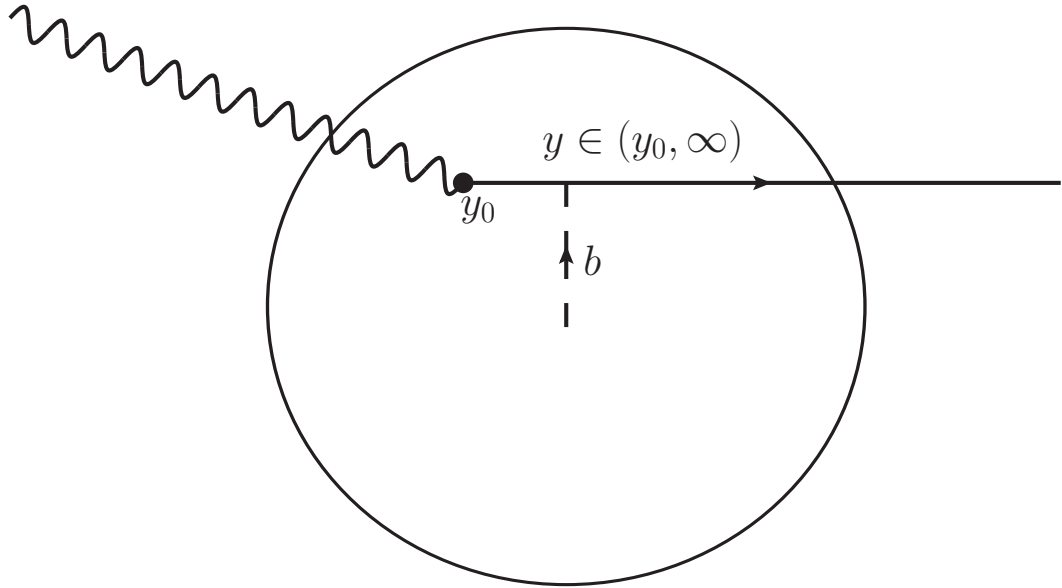


FIG. 16: Illustration of the path integration in DIS. See details in text.

If we neglect the nuclear and impact parameter dependence of the nuclear quark distribution function, the photon-nucleon cross section that produces a quark at (y_0, b) is proportional to the nuclear density distribution $\rho_A(y_0, b)$. Then the averaged mFF should be

$$\tilde{D}(z) = \langle \tilde{D}(z, y_0) \rangle = \frac{\pi}{A} \int_0^\infty db^2 \int_{-\infty}^\infty dy_0 \tilde{D}(z, y_0) \rho_A(y_0, b). \quad (37)$$

In order to calculate the $\tilde{D}(y_0, b)$ for a quark produced at location (y_0, b) , the path integral in the modified splitting functions should be replaced by the following

$$\int dy \hat{q}(y) [\dots] \rightarrow \frac{\hat{q}_0}{\rho_A(0, 0)} \int_{y_0}^\infty dy \rho_A(y, b) [\dots] \quad (38)$$

Shown in Fig. 17 are the calculated nuclear modification factor of π^\pm , K^\pm and $p(\bar{p})$ fragmentation functions with different values of jet transport parameter $\hat{q}_0 = 0.016 - 0.032 \text{ GeV}^2$ as compared to the HERMES experimental data

[49]. The experimental results are presented in terms of multiplicity ratio R_M^h , which represents the ratio of the number of hadrons of type h produced per DIS event for a nuclear target of mass A to that for a deuterium target [48]:

$$\begin{aligned} R_M^h(z, \nu) &= \left(\frac{N^h(z, \nu)}{N^e(\nu)} \Big|_A \right) / \left(\frac{N^h(z, \nu)}{N^e(\nu)} \Big|_D \right) \\ &= \left(\frac{\sum e_f^2 q_f(x) D_f^h(z)}{\sum e_f^2 q_f(x)} \Big|_A \right) / \left(\frac{\sum e_f^2 q_f(x) D_f^h(z)}{\sum e_f^2 q_f(x)} \Big|_D \right). \end{aligned} \quad (39)$$

In the experimental data, each z bin has an averaged value of initial jet energy $\langle E \rangle = \langle \nu \rangle$ and virtuality $\langle Q^2 \rangle$ which we use in the calculation. Since the averaged values of $Q^2 = 2.25 - 2.65$ GeV² in HERMES data are quite small, the suppression factors are apparently sensitive to the value of the initial evolution scale Q_0^2 . In the calculation, we have used $Q_0^2 = 1.0$ GeV². We used the HKN [50] parameterizations as initial condition which extends to down to scale $Q^2 = 1$ GeV². The agreement between the calculation from mDGLAP evolution and the HERMES experimental data [49] are quite well for three nuclear targets in the intermediate region of z values. At large values of z the agreement is not so well maybe due to other effects such as hadronic interaction [51, 52] that we have not taken into account. The calculated modification factors for protons in a large nucleus are also much smaller than the experimental data. This might be related to the non-perturbative baryon transport in hadronic processes [53]. We have so far neglected quark-anti-quark annihilation contribution to the mDGLAP evolution equations. These processes will affect the medium modification of anti-quarks and will likely improve the modification factor for anti-proton distribution.

Shown in Fig. (18) are the calculated nuclear modification factors at fixed z as a function of the initial jet energy E as compared to the HERMES experimental data [49]. Again, each bin of E has an average value of $\langle z \rangle$ and $\langle Q^2 \rangle$ which we also use in the calculation. Similarly as illustrated in the uniform medium (a “brick”), the medium modification of the fragmentation function gradually disappears as the initial jet energy E increases. The agreement between our theory calculations and experimental data is generally good for a range of values of $\hat{q}_0 = 0.016 - 0.032$ GeV², except at lower energy where hadronic absorption might become important. From the combined fit we find the jet transport parameter at the center of large nuclei is $\hat{q}_0 \approx 0.024 \pm 0.008$ GeV²/fm. This value is consistent with the transverse momentum broadening of the Drell-Yan dilepton production in $p + A$ collisions [54–56] $\langle \Delta q_T^2 \rangle = 0.016A^{1/3}$ GeV² which gives an averaged jet transport parameter $\hat{q}_0 = 0.018$ GeV²/fm.

As described in Sec. IV A, we have modeled the initial condition for fragmentation functions in the medium at $Q_0^2 = 1$ GeV² as different from the fragmentation functions in vacuum due to energy loss of parton nearly on shell. Therefore, most of the medium modification to the fragmentation functions come from mDGLAP evolution at low Q^2 while contribution from high Q^2 region is power-suppressed. This will lead to a very weak Q^2 dependence as shown in Fig. 19, where we compared the calculated modification factors for the fragmentation function with experimental data at fixed z and initial jet energy E but as a function of Q^2 . The calculated suppression factors are almost independent of Q^2 , consistent with the experimental data [49]. If one has chosen the initial condition for medium modified fragmentation functions at Q_0^2 as the same as the vacuum one, one would obtain a modification factor that has a too strong Q^2 dependence to be consistent with the experimental data.

VI. SUMMARY

In this paper, we have extended the modified DGLAP evolution equations to include induced gluon radiation for gluon jet and quark-anti-quark pair creation from gluon fusion [43] within the framework of generalized factorization for higher-twist contribution to multiple parton scattering. The effective parton splitting functions are proportional to a path integration of the jet transport parameter \hat{q} over the propagation length. We then numerically solve the coupled mDGLAP equations for medium modified fragmentation functions for different static profile of medium and different values of the jet transport parameter \hat{q} . For a “brick” profile, we have studied the shower parton distributions within a jet during its propagation through the medium and relate the change of momentum fraction carried by the valence quark as the effective energy loss of a propagating quark. We have systematically studied the energy, medium length and virtuality dependence of the medium modified fragmentation functions. Because of the inclusion of induced pair creation and different splitting functions for gluon and quark jets in the mDGLAP evolution, we found that the modification factors are different for gluon, valence quark and sea quark fragmentation functions.

We also applied the mDGLAP evolution to quark propagation in the deeply inelastic scattering (DIS) of a large nucleus and found the calculated nuclear modification of the effective fragmentation functions in good agreement with experimental data in the intermediate z region. In modeling the initial condition for modified fragmentation functions, we have chosen to include medium induced radiation and parton energy loss below the initial scale Q_0^2 . In this case,

most of the medium modification comes from mDGLAP evolution in the low Q^2 region while large Q^2 contribution is power-suppressed. This leads to a weak Q^2 dependence of the medium modification of the fragmentation functions which is consistent with the experimental data in DIS.

Acknowledgement

We would like to acknowledge helpful discussions with A. Majumder. X.N.W thanks the hospitality of the Physics Department of Shandong University during the completion of this work. This work is supported by the Director, Office of Energy Research, Office of High Energy and Nuclear Physics, Divisions of Nuclear Physics, of the U.S. Department of Energy under Contract No. DE-AC02-05CH11231 and National Natural Science Foundation of China under Project Nos. 10525523.

-
- [1] X. N. Wang and M. Gyulassy, Phys. Rev. Lett. **68**, 1480 (1992).
 - [2] M. Gyulassy and X. N. Wang, Nucl. Phys. B **420**, 583 (1994).
 - [3] R. Baier, Y. L. Dokshitzer, A. H. Mueller, S. Peigne and D. Schiff, Nucl. Phys. B **484**, 265 (1997)
 - [4] U. A. Wiedemann, Nucl. Phys. B **588**, 303 (2000)
 - [5] M. Gyulassy, P. Levai and I. Vitev, Nucl. Phys. B **594**, 371 (2001)
 - [6] X. F. Guo and X. N. Wang, Phys. Rev. Lett. **85**, 3591 (2000)
 - [7] X. N. Wang and X. F. Guo, Nucl. Phys. A **696**, 788 (2001)
 - [8] X. N. Wang, Phys. Rev. C **58**, 2321 (1998)
 - [9] X. N. Wang, Phys. Rev. C **61**, 064910 (2000)
 - [10] X. N. Wang, Z. Huang and I. Sarcevic, Phys. Rev. Lett. **77**, 231 (1996)
 - [11] X. N. Wang and Z. Huang, Phys. Rev. C **55**, 3047 (1997)
 - [12] F. Arleo, JHEP **0609**, 015 (2006).
 - [13] T. Renk, Phys. Rev. C **74**, 034906 (2006)
 - [14] H. Zhang, J. F. Owens, E. Wang and X. N. Wang, Phys. Rev. Lett. **103**, 032302 (2009)
 - [15] G. Y. Qin, J. Ruppert, C. Gale, S. Jeon and G. D. Moore, Phys. Rev. C **80**, 054909 (2009)
 - [16] X. N. Wang, Phys. Lett. B **595**, 165 (2004)
 - [17] H. Z. Zhang, J. F. Owens, E. Wang and X. N. Wang, Phys. Rev. Lett. **98**, 212301 (2007).
 - [18] A. Majumder, E. Wang and X. N. Wang, Phys. Rev. Lett. **99**, 152301 (2007)
 - [19] K. Adcox *et al.*, Phys. Rev. Lett. **88**, 022301 (2002).
 - [20] C. Adler *et al.*, Phys. Rev. Lett. **89**, 202301 (2002).
 - [21] C. Adler *et al.*, Phys. Rev. Lett. **90**, 082302 (2003).
 - [22] J. Adams *et al.*, Phys. Rev. Lett. **97**, 162301 (2006); A. M. Hamed, J. Phys. G **35**, 104120 (2008);
 - [23] J. Frantz, arXiv:0901.1393 [nucl-ex].
 - [24] I. Vitev and M. Gyulassy, Phys. Rev. Lett. **89**, 252301 (2002)
 - [25] K. J. Eskola, H. Honkanen, C. A. Salgado and U. A. Wiedemann, Nucl. Phys. A **747**, 511 (2005)
 - [26] S. Turbide, C. Gale, S. Jeon and G. D. Moore, Phys. Rev. C **72**, 014906 (2005)
 - [27] For a comparison of different models and their phenomenology, see A. Majumder, arXiv:nucl-th/0702066; to be published in the proceedings of Quark Matter 2006, Shanghai, Nov. 14-19, 2006.
 - [28] E. Wang and X.-N. Wang, Phys. Rev. Lett. **89**, 162301 (2002).
 - [29] P. Aurenche, M. Fontannaz, J. P. Guillet, B. A. Kniehl and M. Werlen, Eur. Phys. J. C **13**, 347 (2000)
 - [30] J. F. Owens, Phys. Rev. D **65**, 034011 (2002)
 - [31] H. Baer, J. Ohnemus and J. F. Owens, Phys. Rev. D **42**, 61 (1990).
 - [32] Y. L. Dokshitzer, Sov. Phys. JETP **46**, 641 (1977) [Zh. Eksp. Teor. Fiz. **73**, 1216 (1977)]. V. N. Gribov and L. N. Lipatov, Sov. J. Nucl. Phys. **15**, 438 (1972) [Yad. Fiz. **15**, 781 (1972)]. G. Altarelli and G. Parisi, Nucl. Phys. B **126**, 298 (1977).
 - [33] R. D. Field, *Application of Perturbative QCD*, Vol. 77 of Frontiers in Physics Lecture Series (Addison-Wesley, Reading, MA, 1989).
 - [34] N. Armesto, L. Cunqueiro, C. A. Salgado and W. C. Xiang, JHEP **0802**, 048 (2008)
 - [35] K. Zapp, J. Stachel and U. A. Wiedemann, arXiv:0812.3888 [hep-ph].
 - [36] A. Majumder, arXiv:0901.4516 [nucl-th].
 - [37] B. W. Zhang and X. N. Wang, Nucl. Phys. A **720**, 429 (2003)
 - [38] L. D. Landau and I. Pomeranchuk, Dokl. Akad. Nauk Ser. Fiz. **92** (1953) 735.
 - [39] A. B. Migdal, Phys. Rev. **103**, 1811 (1956).
 - [40] J. Osborne and X. N. Wang, Nucl. Phys. A **710**, 281 (2002)
 - [41] J. Casalderrey-Solana and X. N. Wang, Phys. Rev. C **77**, 024902 (2008)
 - [42] X. N. Wang, Phys. Lett. B **650**, 213 (2007)
 - [43] A. Schafer, X. N. Wang and B. W. Zhang, Nucl. Phys. A **793**, 128 (2007)

- [44] G. P. Salam and J. Rojo, *Comput. Phys. Commun.* **180**, 120 (2009)
- [45] M. Luo, J. W. Qiu and G. Sterman, *Phys. Lett. B* **279**, 377 (1992). M. Luo, J. w. Qiu and G. Sterman, *Phys. Rev. D* **50**, 1951 (1994). M. Luo, J. W. Qiu and G. Sterman, *Phys. Rev. D* **49**, 4493 (1994).
- [46] H. Zhang, J. F. Owens, E. Wang and X. N. Wang, *Phys. Rev. Lett.* **98**, 212301 (2007)
- [47] R. Baier, Y. L. Dokshitzer, A. H. Mueller, S. Peigne and D. Schiff, *Nucl. Phys. B* **484**, 265 (1997)
- [48] A. Airapetian *et al.* [HERMES Collaboration], *Eur. Phys. J. C* **20**, 479 (2001) V. Muccifora [HERMES Collaboration], *Nucl. Phys. A* **715**, 506 (2003)
- [49] A. Airapetian *et al.* [HERMES Collaboration], *Nucl. Phys. B* **780**, 1 (2007)
- [50] M. Hirai, S. Kumano, T. H. Nagai and K. Sudoh, *Phys. Rev. D* **75**, 094009 (2007)
- [51] B. Z. Kopeliovich, *Phys. Lett. B* **243**, 141 (1990).
- [52] F. Arleo, *Eur. Phys. J. C* **30**, 213 (2003)
- [53] D. Kharzeev, *Phys. Lett. B* **378**, 238 (1996)
- [54] X. F. W. Guo, *Phys. Rev. D* **58**, 114033 (1998)
- [55] X. F. Guo, J. W. Qiu and X. F. Zhang, *Phys. Rev. D* **62**, 054008 (2000)
- [56] P. L. McGaughey, J. M. Moss and J. C. Peng, *Ann. Rev. Nucl. Part. Sci.* **49**, 217 (1999)

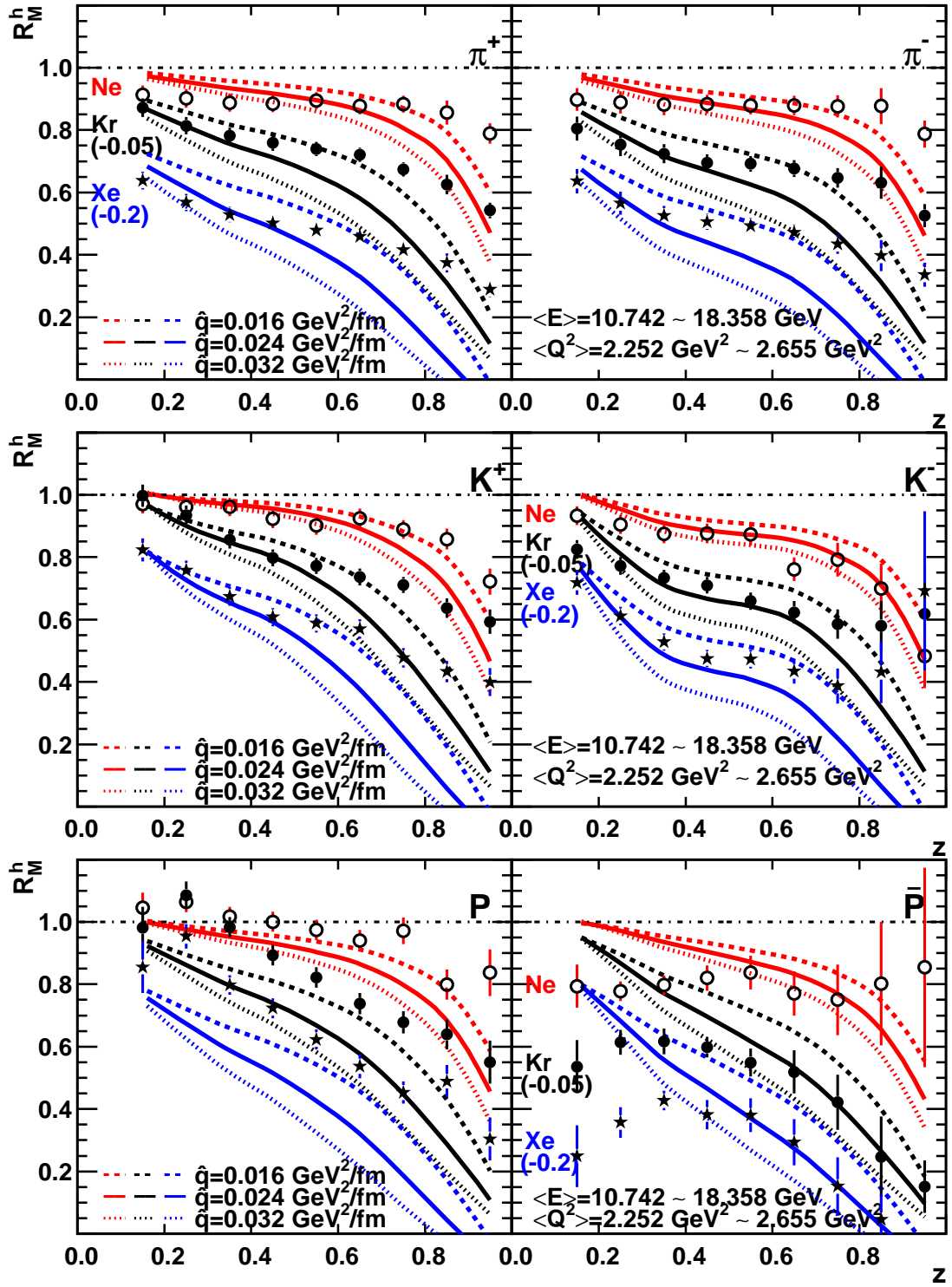


FIG. 17: (color online) The modified multiplicity ratios as a function of z with different values of the jet transport parameter \hat{q}_0 compared with the HERMES [49] data for Ne, Kr and Xe targets. For clear presentation the modification factors for different targets have been shifted vertically by some value (Kr by -0.05 and Xe by -0.2).

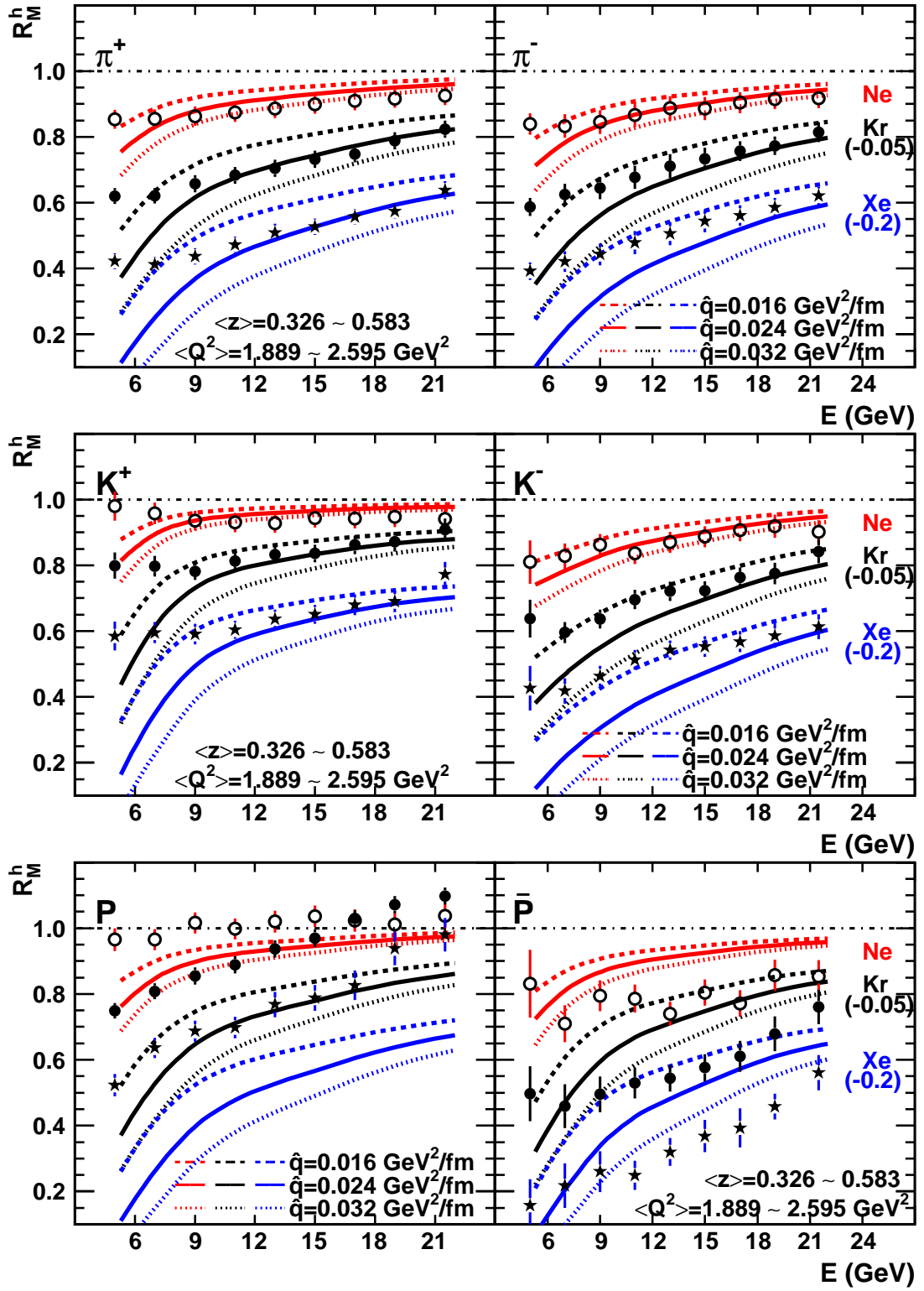


FIG. 18: (color online) The energy dependency of the nuclear modification factors with different values of the jet transport parameter \hat{q}_0 compared with the HERMES [49] data for Ne, Kr and Xe targets. For clear presentation the modification factors for different targets have been shifted vertically by some value (Kr by -0.05 and Xe by -0.2).

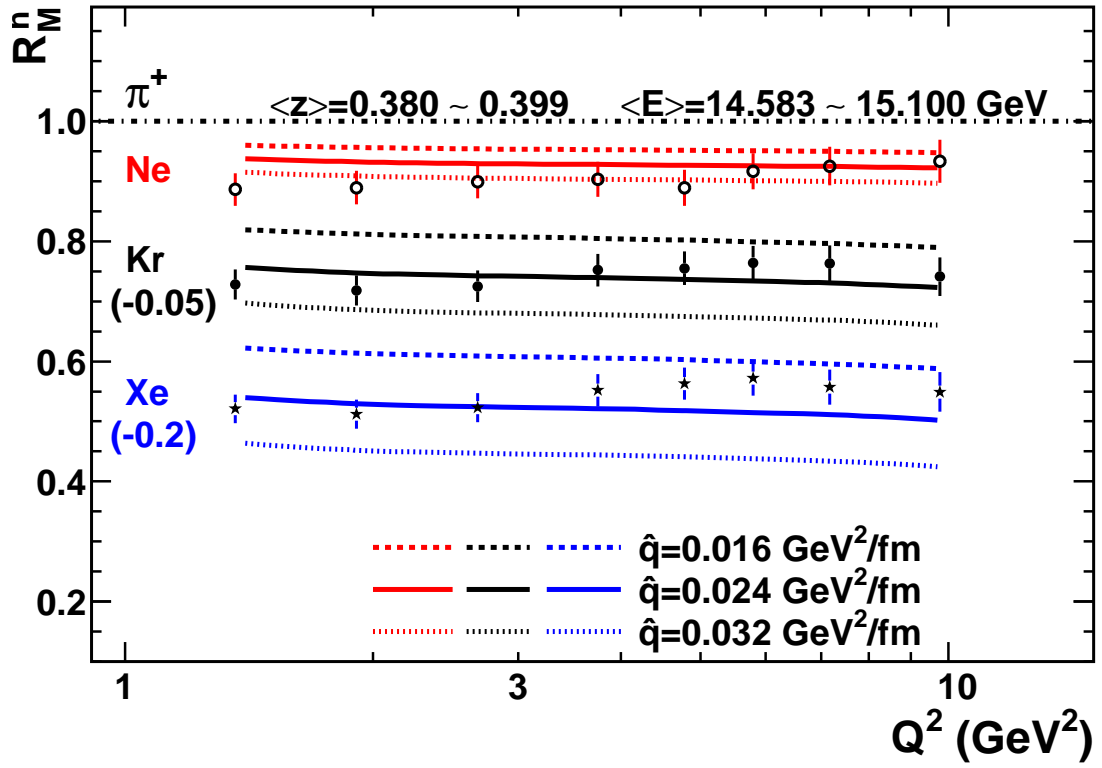


FIG. 19: (color online) Comparison of the modified multiplicity ratios as a function of Q^2 at fixed value of z and jet energy E with the HERMES [49] data for Ne , Kr and Xe targets. For clear presentation the modification factors for different targets have been shifted vertically by some value (Kr by -0.05 and Xe by -0.2).